FACILE SYNTHESIS, SOLUBLIZATION STUDIES AND ANTI-INFLAMMATORY ACTIVITY OF AMORPHOUS ZINC(II) CENTERED ALDIMINE COMPLEXES**

Uzma ALI,[a] Aneela MAALIK,[b] Muhammad Babar TAJ,[c,d,*] Ahmad RAHEEL,[a,*]
Ahmad Kaleem QURESHI,[d] Muhammad IMRAN,[c] Muhammad SHARIF,[c]
Syed Ahmad TIRMIZI,[a,*] Sadia NOOR,[e,*] and Heba ALSHATER[f]

[a]Department of Chemistry, Quaid-e-Azam University Islamabad 44000, Pakistan
[b]Department of Chemistry, Comsats University, Park Road, Chak Shahzad Islamabad 44000, Pakistan
[c]Department of Chemistry, Islamia University Bahawalpur 63100, Pakistan.
[d]Department of Chemistry, University of Sahiwal 57000, Pakistan.
[d]Department of Chemistry, University of Agriculture, Faisalabad 38000, Pakistan
[f]Department of Forensic Medicine and Clinical Toxicology, Menoufia University Menofia 32871, Egypt

In this study, Zn(II) centered complexes with aldimine derivatives were synthesized using green solvent, polyethylene glycol (PEG-400) and amorphous complexes were characterized by FT-IR, multinuclear (^{1}H and ^{13}C NMR), elemental and thermal analysis. Thermogravimetric analysis indicated the extended thermal stability of the synthesized complexes. All the Zn(II) complexes show very significant photoexcitation in the range of 318 – 384 nm and photoemission in the range of 502 – 562 nm. Among all the complexes, Zn(II) complex (3Zn) showed minimum band gap value, 2.35 eV. These amorphous complexes have been reported for their wide applications in biomedical sciences. The synthesized aldimine ligands and Zn(II) complexes were investigated for anti-inflammatory activity and these complexes showed more anti-inflammatory potential than the corresponding aldimine ligands. The solubilization of zinc complexes in sodium dodecyl sulphate was also investigated to reveal the interaction of metal complexes by using UV-Visible spectroscopy and electrical conductivity measurements.
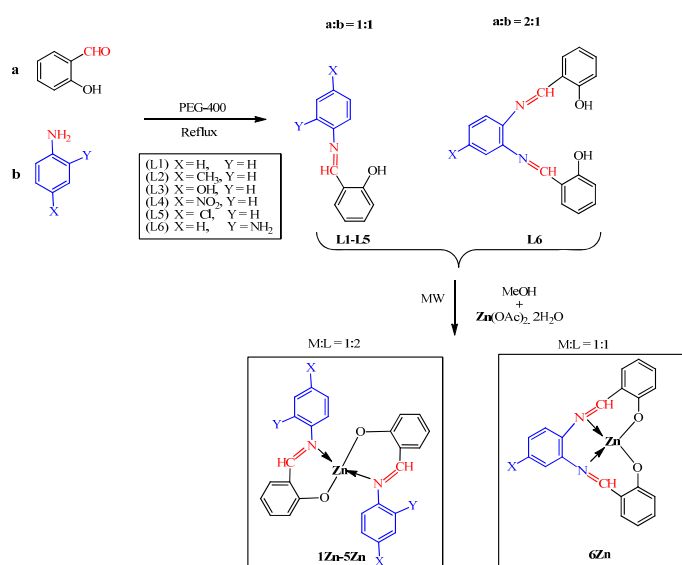
INTRODUCTION

Aldimines belong to a very vital class of compounds due to their wide range of applications in the field of medicine and they also act as ligands coordinating to various transition metals.[1] The aldehydes with extended conjugation (aromatic aldehydes) give rise to stable aldimines derivatives (Schiff base) and they form more readily as compared to ketimines.[2] Their contributions to

coordination chemistry cannot be taken for granted. The metal complexes in comparison with the organic compounds offer a variety of electronic structures linked with the coordination sphere, oxidation states and electronic configuration of metal.[3] They show many types of transitions including low energy ligand-to-metal charge transfer (LMCT), metal to ligand charge transfer (MLCT) and intra-ligand charge transfer (ILCT).[4] The incorporation of metals within aldimine moieties bestows them some degree of antitumor,[5] antifungal,[6] antibacterial[7] and anti-inflammatory activities.[8] The process of solubilization is a very valuable tool in understanding drug/excipient interaction with biomembranes and playing a vital role in many industrial and biological processes.[8] The micelle formation is the most distinctive property of surfactants which allow metal complexes or drugs to solubilize to the greater extent.[8]

The structural features of these compounds also enhance several interesting properties such as photoluminescence.[9] The metal-aldimine complexes, particularly Zn(II) centered salicylaldiminato compounds have also been previously reported for their use as greenish-white, blue, and red-light emitters in organic optoelectronics due to their high efficacy and stability.[10] The ligand field stabilization effect and d^{10} configuration of the metal centered aldimine complexes mask and hinder the stereochemistry grooves.[11] Due to the absence of d-d or metal-to-ligand transitions, Zn(II) complexes are optically more active, transparent than other related d^n analogues.[12]

Keeping in view the literature, we are herein reporting the synthesis of six aldimine ligands and their Zn(II) complexes. The photoluminescence, anti-inflammatory and solubilizations parameters of synthesized compounds have also been discussed.

RESULTS AND DISCUSSION

Characterization of synthesized zinc complexes

The green synthesis of aldimine ligands and their Zn(II) complexes are represented in Scheme 1. The synthesized Zn(II) complexes were insoluble in common organic solvents but soluble in DMSO and DMF. Many attempts were made to get single crystals of these complexes but unfortunately, we could not succeed. In the absence of single-crystal determination, the structures and geometry of zinc complexes were confirmed and characterized by

elemental analysis along with other spectroscopic and thermal analyses. The elemental analyses showed that the metal-to-ligand ratio of 1:2 in all the complexes except 6Zn (1: 1). The Zn(II) complexes were amorphous, non-hygroscopic and coloured.

FTIR analysis

The bonding of the aldimine to Zn(II) ions was observed by a careful comparison of the infrared spectra of the Zn(II) complexes with those of the corresponding free aldimine ligands. A strong characteristic band appeared at 1603–1615 cm^{-1} because of C=N stretching vibration, which indicated aldimine formation. A sharp peak for C-O stretching vibration of the phenolic hydroxyl group was spotted at 1255–1278 cm^{-1}. Presence of O-H stretching vibration at 3433–3494 cm^{-1} indicated the presence of water in the samples. This was due to the moisture contents in the samples. As these moisture contents have not appeared in the further analysis which has done after drying the sample for 2h in the oven.

In IR spectra of complexes, the C=N stretching vibration was observed to shift towards lower wavenumber indicated the presence of free ligand. This feature can be ascribed to the withdrawal of electron density from N atom owing to coordination. C-O stretching vibration became weaker in intensity in the spectra of complexes. New peaks observed in the regions of 434–516 cm^{-1} and 531–587 cm^{-1}, were assigned to Zn-O and Zn-N stretching vibrations, respectively. These features suggested that the binding takes place through imine nitrogen and the phenolic oxygen atom of the aldimine to the Zn(II) ion forming tetrahedral geometry.

Structural assignments by the mean NMR

^{1}H NMR spectra of all the aldimines and their Zn(II) complexes were recorded in DMSO-d_6. All the protons in the spectra were identified and the total number of calculated protons was found in good agreement with the proposed structures. The comparison of ^{1}H NMR data of aldimine ligands and Zn(II) complexes showed that the peak of the phenolic proton at 12.59–13.43 ppm was observed in the spectra of free ligands. This peak was absent in the spectra of these complexes which suggests complexation through the phenolic oxygen. Singlet peak at 8.62–8.65 ppm present in the spectra of

aldimine **L2** shifted toward the high field and appeared at 8.37 ppm in the spectrum of Zn(II) complex. Aromatic protons gave multiple peaks in the ligands and a doublet with J values ranging from 7.8–8.4 Hz. In proton NMR spectrum of Zn(II) complex of aldimine **L2** the multiplets then shifted to 7.20–7.23, 6.94–7.08 and 6.64–6.70 ppm and the peak of methyl proton shifted to 2.29 ppm owing to the coordination of zinc atom with the ligand.

^{13}C NMR spectra of the complexes were also recorded in DMSO-d$_6$. In ^{13}C NMR spectra, the signal of the carbon attached to the hydroxyl group in the ligands was observed at 161–165.4 ppm, which shifted downfield at 171.32 and 171.17 ppm respectively after complexation with the Zn(II) ions, which suggested bonding through this oxygen to the central zinc atom. The azomethine (C=N) carbon in ligands gave a signal at 160.4–161.3 ppm which shifted down the field in the Zinc (II) complexes and appeared at 169.68 and 169.05 ppm, respectively. This deshielding of azomethine carbon on complexation further supported the involvement of nitrogen in complexation leading to the tetrahedral geometry of Zn(II) complexes.

Thermal Analysis

The thermal analysis data of the Zn(II) complexes is given in Table 1. The presence of lattice or coordinated water molecules was determined from TG curves. The weight losses of complexes were calculated within the temperature range at which the water molecules were removed. The values were used in the calculation of the number of water molecules attached to the metal complexes. The calculated weight loss due to water was calculated from the suggested molecular weight based on the Elemental Analysis data. The decomposition temperatures of the Zn(II) complexes were determined from the TG curves.

Optical Properties

Optical Absorption Properties

Absorption spectra of Zn(II) complexes were recorded in dilute chloroform solution (10^{-6} mol L^{-1}). The positions of absorption bands are shown in Table 2. Three absorption bands were observed with λ_{max} at 236–292, 316–327 and 337–391 nm, respectively. The high energy absorption bands were assigned to the spin-allowed singlet intra ligand (^{1}IL) transition of the aldimine ligand. Zn(II) was not involved in electronic transitions in the UV-visible spectral region, and those absorptions in this region were assigned to ligand-centered (LC) π-π^* transitions of the aldimine ligands. From these assignments, it was concluded that the HOMOs of the aldimine ligand systems were localized on the phenoxide units and the LUMOs were localizes at the imine groups.

Table 1

Thermal Analysis Data of Zn(II) Complexes

Complex	Decomp. steps	Water content		% Wt. loss due to water		Decomp. T (°C)	Peak T (°C)
		Calcd.	Found	Calcd.	Found		
1Zn	2	-	-	-	-	281	389,529
2Zn	2	0.57	2.96	2.06	9.92	272	110,403,559
3Zn	3	1.09	1.75	3.86	6.06	238	187,354,539
4Zn	2	0.36	-	1.18	-	300	357,524,
5Zn	2	1.68	1.31	7.42	5.86	430	192,546
6Zn	2	3.62	3.19	12.82	11.46	384	192,546

Table 2

UV-visible Absorption Data of Zn(II) Complexes

Complex	π-π^* phenyl (nm)	π-π^* C=N (nm)	π-π^* ^{1}IL (nm)
1Zn	268	316	337
2Zn	275	321	342
3Zn	268	324	343
4Zn	236	322	351
5Zn	292	327	391
6Zn	274	318	367

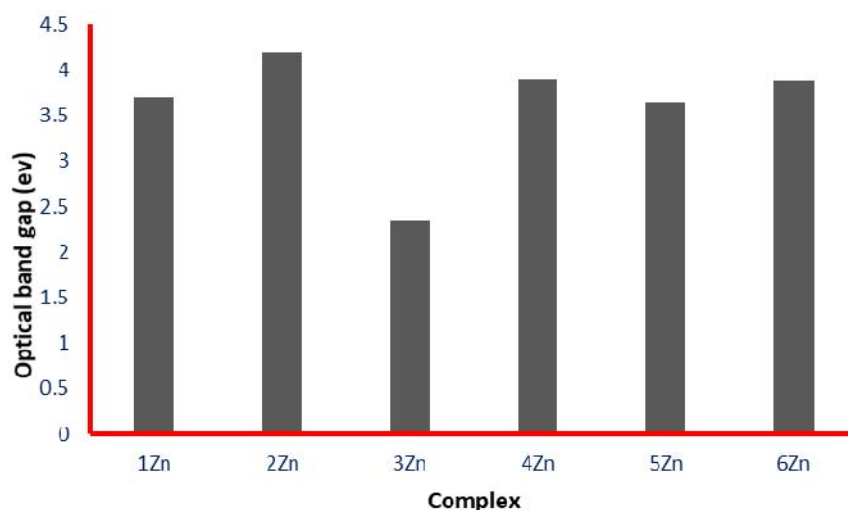| Complex	Excitation λ (nm)	Emission λ (nm)	Emission colour
1Zn	335	533	Green
2Zn	318	484	Blue
3Zn	337	465	Greenish blue
4Zn	326	562	Yellowish green
5Zn	394	502	Bluish-green
6Zn	369	536	Bluish-green

Fig. 1 – Optical Band Gaps of Zn(II) Complexes.

Optical Excitation and Emission Properties

The photoluminescence (PL) emission for the complexes in chloroform solution from blue to yellow span was assigned to intra ligand $(\pi^{*}-\pi)$ fluorescence. The excitation and emission wavelengths are summarized in Table 3.

As observed in the optical absorption results, the LUMO of the Zn(II) complexes were localized at the imine group. The LUMO level was destabilized with the addition of the electron-donating group. As a result, blue shifts in the emission maxima of 2Zn and 3Zn were observed concerning 1Zn. Whereas the redshift is observed in the emission maximum of 4Zn as compared to 1Zn.

Optical Band Gap Determination

Figure 2 shows the analysis of the optical absorption band edge of Zn(II) complexes in chloroform solutions. The optical bandgap of the films was determined by applying the Tauc model [13], which was firstly but empirically proposed by Jellison and Modine in 1996.

The curves were determined by optical absorption spectra with the relationship following equation 10:

$$ah\nu = B(h\nu - E_g)^n$$

where a is absorption coefficient; h is Plank's constant; ν is frequency, E_g is optical band gap; B is constant relation to the material; n=1/2 under the assumption of direct inter-band transition. The optical absorption coefficient, a, is calculated using the relation; $a(\lambda) = 2.303A(\lambda)/L$, where a=absorption coefficient in m^{-1}, A=absorbance in a.u., L=path length in meter.

Photon energy in eV was calculated using the relation: $E = h\nu = hc/\lambda = 1240(nm) \, eV/ \, \lambda(nm)$.

The optical band gap was evaluated by the energy value of the crossover point of the linear absorption band edge and energy axis. The values of the approximate optical band gaps E_g obtained from the graphical relation are depicted in Figure 1.

As mentioned earlier the HOMOs of the aldimine ligand systems were localized on the phenoxide units and the LUMOs on the imine group and the LUMO level destabilized in the presence of electron-donating group and in turn the band gap between HOMO and LUMO levels was supposed to increase.

Anti-inflammatory activity (bovine serum albumin test)

BSA denaturation assay was employed to know the anti-inflammatory potential of aldimine ligands

and their Zn(II) complexes (Figure 2). Broadly, the Zn(II) complexes showed more anti-inflammation than their corresponding aldimine ligands. The Zn(II) complex 6Zn show maximum inhibition of $88.27 \pm 2.0\%$ at a maximum concentration of 500 mg mL^{-1}. This better inhibition as compared with the standard drug diclofenac sodium was possibly due to the strong coordination of metal with the

ligand **L6**. This could also be attributed to the tetradentate nature of the ligand **L6** causing stronger coordination with zinc as compared to other bidentate ligands (**L1-L5**). The results from our investigation were found in agreement with previously reported studies, which also indicated the enhancement of the anti-inflammatory activity of ligands upon coordination with the metal ions.
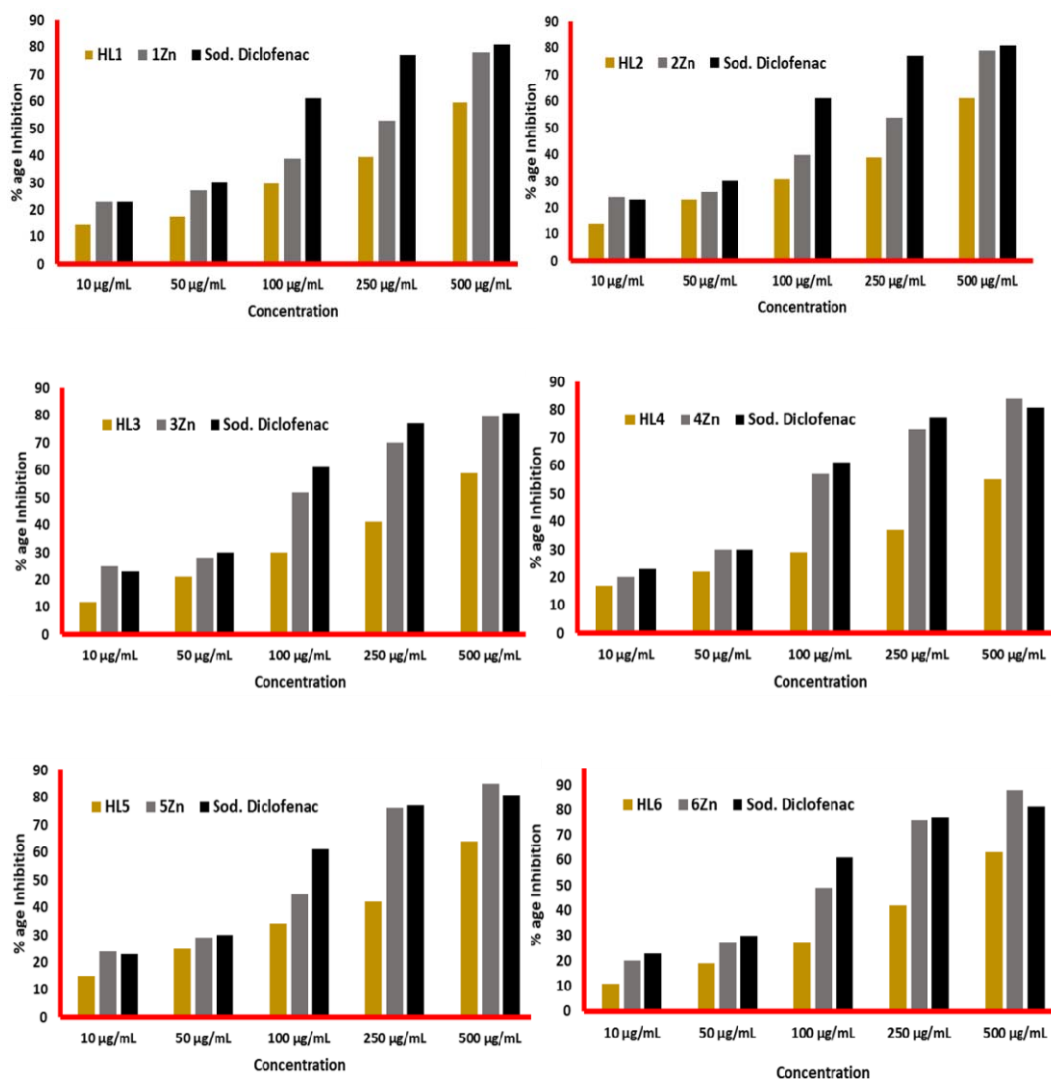

Fig. 2 – Anti-inflammatory evaluation of ligands (**L1- L6**) and their zinc complexes (**1Zn-6Zn**).

Mechanistically this enhancement of the anti-inflammatory activity of Zn(II) complexes could be explained through Overtone's concept of cell permeability and Tweedy's theory of chelation.[14] According to Overtone's concept, liposolubility is the major factor controlling the anti-inflammatory activity.[15] As the lipid membrane around the cell allows the passage of only lipid-soluble molecules. On the other hand, in chelation polarity of the metal ion diminishes due to the overlapping of the ligand orbital and partial sharing of the positive

charge of the metal ion with donor groups. Moreover, delocalization of π-electrons of metal chelate enhances the lipophilicity which results in the high penetration of metal complexes into the lipid membrane and blocks the metal-binding sites in the enzymes of pathogens. These metal complexes also disrupt the cell respiration process and thus block the proteins synthesis, which inhibit the growth of the pathogens.[16] In general, metal complexes are more active than ligands as they may serve as principal cytotoxic species.

Solubilization of synthesized zinc complexes in micellar media of SDS

The solubilization of zinc complexes (1Zn-6Zn) in the micellar media of SDS was investigated through conductometric and spectroscopic measurements.

UV-Visible spectroscopic measurements

Interaction of zinc complexes with SDS molecules was revealed by measuring simple and differential absorbance by UV-Visible spectroscopy. The values of maximum absorbance (λ_{max}) zinc complexes (1Zn-6Zn) in the absence and presence of the surfactant were recorded to assess the extent of interaction, as could be seen in Table 4. It was envisaged that the prevailing electrostatic and hydrophobic interactions influenced the molecules of zinc complexes to incorporate in the proximal regions of SDS micelles. There was a gradual increment in the absorption with increasing surfactant concentrations and the molecules of complexes incessantly interacted within the micelles hence their critical micellar concentration (CMC) increased. There was a bathochromic shift which indicated interactions of complexes with surfactant molecules in the micellar form.

Differential absorbance provides insight into the nature and existence of interactions of surfactants and complex molecules and provides understanding about their partitioning and binding trends in the micellar media. Among all complexes, 6Zn showed the highest tendency to partition towards the micelles of SDS while 4Zn was the on the lowest side. The partitioning law governed the behaviour of zinc complexes between aqueous and micellar media and partition coefficient (K_x) helps in this evaluation (Table 5).

The plots representing simple (A) and differential absorbance (ΔA) of zinc complex against surfactant concentration to estimate the variations in CMC are shown in Figures 3 and 4.

There was an increasing trend for the CMC of surfactant (SDS) in the presence of zinc complexes due to their structure breaking effect. The solubilization parameters are summarized in Table 5. The penetration of zinc complex molecules into the micellar regions of SDS increased the values of CMC in comparison to pure SDS. The involvement of intermolecular hydrogen bonding between water and zinc complex molecules caused their adsorption in the periphery of surfactant micelles.

Table 4

The shift in the maximum absorbance of metal complexes in aqueous and micellar media

Complex	λ_{max} (nm) (aqueous media)	λ_{max} (nm) (SDS micellar media)
1Zn	268	293
2Zn	274	307
3Zn	347	376
4Zn	336	367
5Zn	390	421
6Zn	309	343

Table 5

Partitioning and binding parameters of zinc complexes in the micellar media of SDS

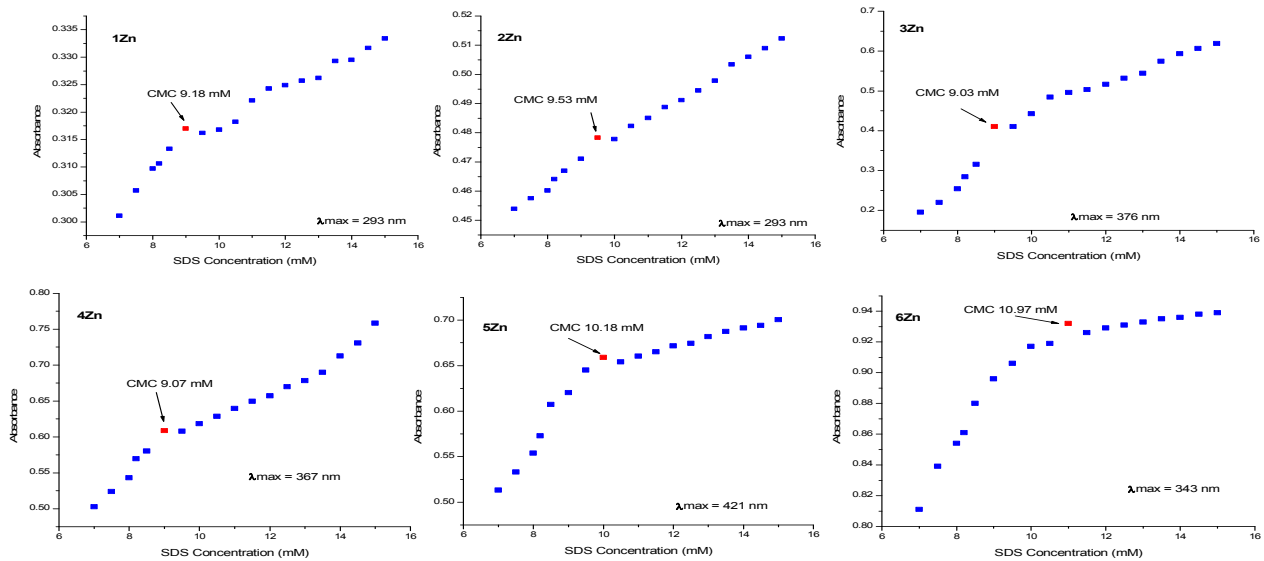| Complex	K_x (dm^3/mol)	ΔG_p (kJ/mol)	K_b (dm^3/mol)	ΔG_b (kJ/mol)
1Zn	13400	-23.54	240	-13.58
2Zn	2510	-19.39	70	-10.53
3Zn	2150	-19	58.5	-10.08
4Zn	2000	-18.82	80	-10.85
5Zn	5940	-21.53	163	-12.61
6Zn	19600	-24.49	367	-14.62

Fig. 3 – Simple absorbance of zinc complexes in the micellar media of SDS.
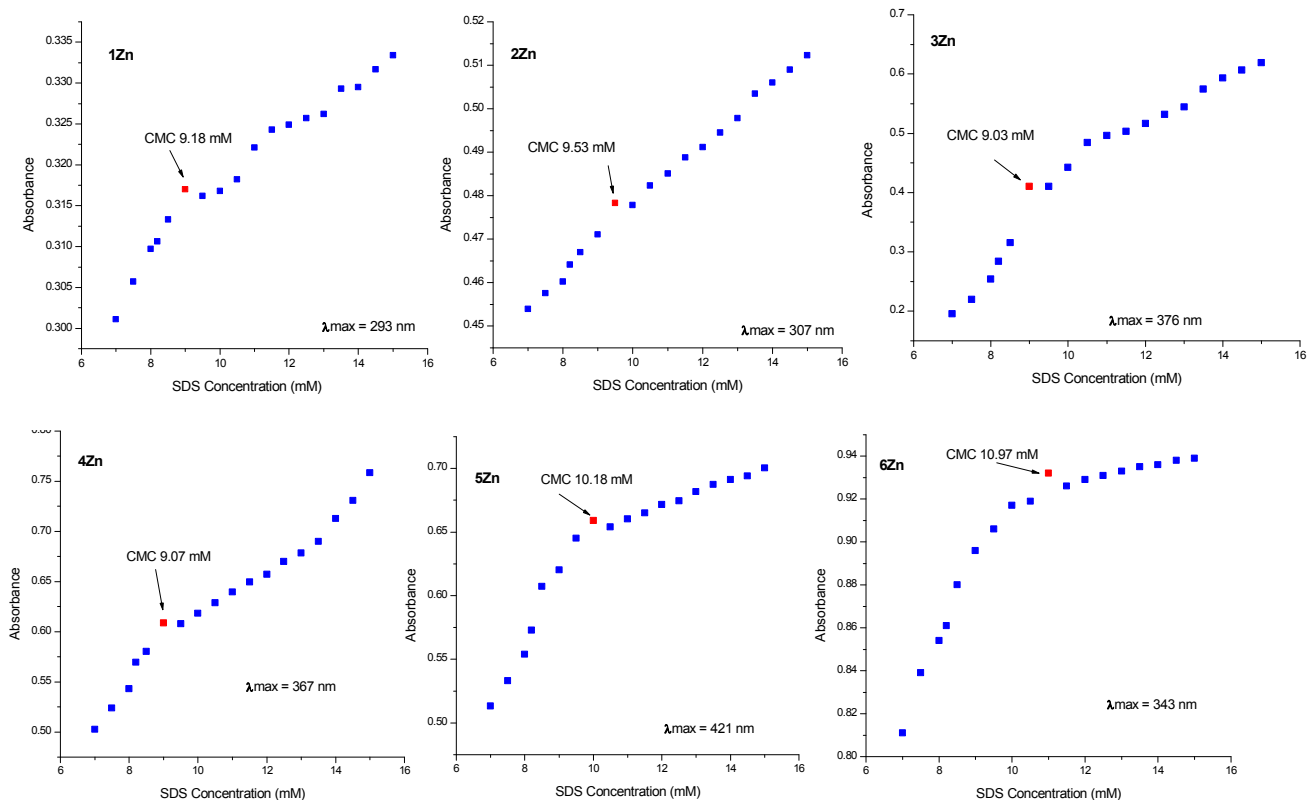

Fig. 4 – Differential absorbance of zinc complexes in the micellar media of SDS.

Electrical conductivity measurements

The thermodynamic parameters and the values CMC of zinc complexes (1Zn-6Zn) in the presence of SDS were explored using electrical conductivity data. It was observed that on gradual dilution, there was a noticeable change in the conductivity of the solutions. The experimental data was then compiled and calculated using equations 6–9 given in the experimental section. The results were graphically presented as plots of electrical conductivity (EC) against surfactant concentrations (CS) as elaborated in Figure 5. The value critical micellar concentration (CMC) was calculated from the point of intersection on two straight lines and with increasing temperature of solutions, this value increased.
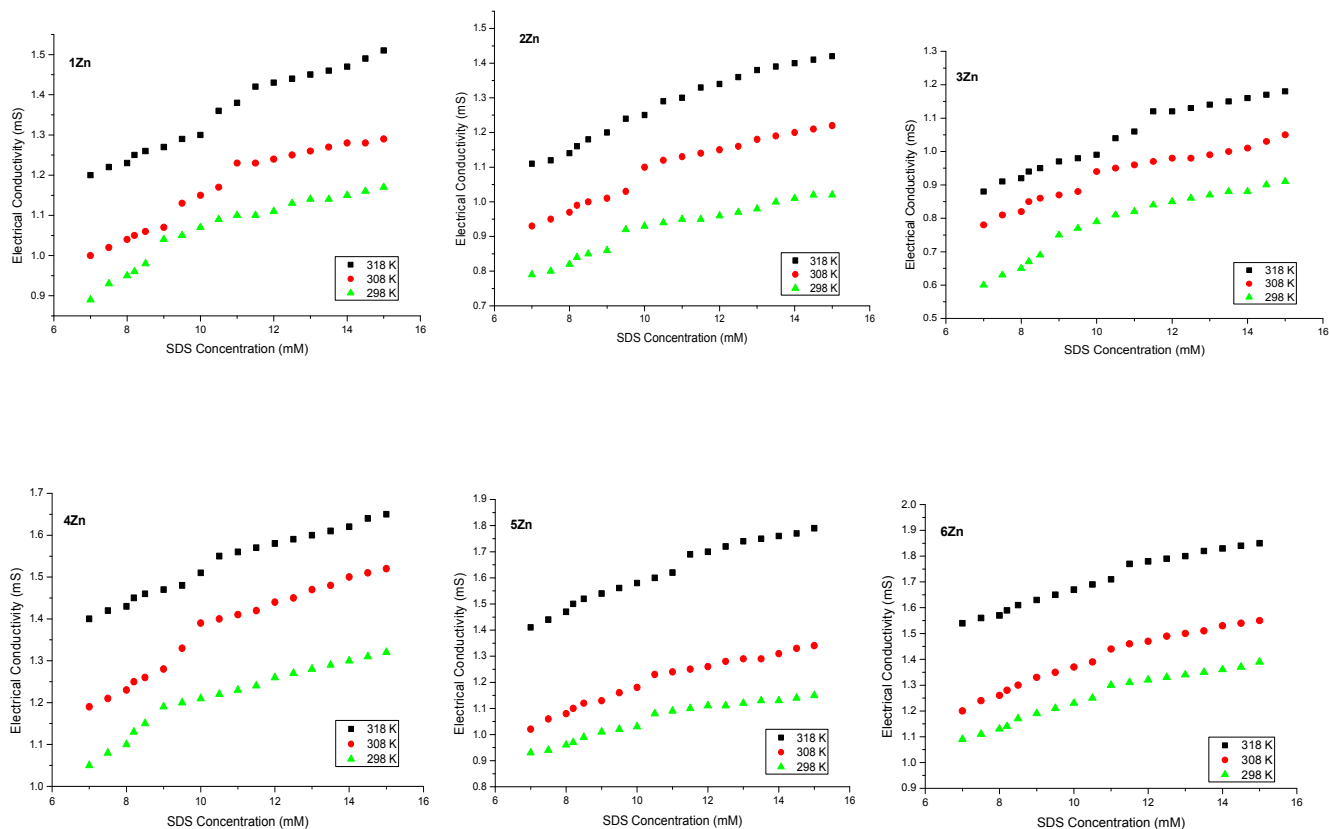
Fig. 5 – Graphical representation of electrical conductivity at various temperatures.

Table 6

Thermodynamic attributes of zinc complexes in the micellar media of SDS

Complex	T (^{o}C)	CMC (mM)	ΔG_m (kJmol^{-1})	ΔH_m (kJmol^{-1})	ΔS_m (Jmol^{-1}K^{-1})	β
1Zn	25	9.14	-36.28	-8.71	92.52	0.29
	35	9.51	-29.74	-7.96	70.71	0.54
	45	10.5	-33.10	-7.78	79.65	0.66
2Zn	25	9.46	-34.46	-6	95.52	0.40
	35	10.02	-32.12	-6.17	84.23	0.46
	45	10.48	-35.02	-6.2	90.63	0.55
3Zn	25	8.96	-36.02	-6.80	98.09	0.34
	35	9.8	-31.01	-6.86	78.43	0.43
	45	10	-35.87	-6.51	92.34	0.59
4Zn	25	9	-36.33	-10.0	88.38	0.32
	35	10.03	-31.58	-10.03	69.99	0.42
	45	10.56	-35.73	-9.69	81.88	0.57
5Zn	25	10.12	-35.17	-5.91	98.19	0.35
	35	11.99	-32.84	-5.89	87.50	0.46
	45	12.04	-34.62	-6.08	89.74	0.5
6Zn	25	11	-33.14	-5.6	92.41	0.43
	35	11.24	-32.42	-5.77	86.53	0.49
	45	11.59	-33.88	-6.05	87.51	0.51

There was significant interaction in zinc complex with the micelles of surfactant and the thermodynamic parameters are summarized in Table 6. The negative values of ΔH_m and ΔG_m indicated that micellization was an exothermic process and it favoured the stability and spontaneity of the system. This process was also entropy-driven as could be seen in the positive

values of entropy (ΔS_m), due to significantly transferring hydrophobic tails from aqueous to the core micellar zone.

Comparative interaction of selected metal complexes with SDS

The results obtained from UV-Visible spectroscopy and those of electrical conductivity were in close agreement in terms of CMC. The highest partitioning coefficient (19600 dm^3/mol) and binding constant (367 kJ/mol) of 6Zn/SDS system among other complexes, indicated it highest partitioning between micellar and aqueous medium. As a result of this phenomenon of partitioning and binding, 6Zn molecules remained near the peripheral zone

of SDS micelles while other complexes positioned them in their corresponding regions depending on their partitioning and binding values. Though the micellization phenomenon has not been fully explained, yet we can assign some generalizations to this process. The highest negative value ΔG_p (-24.49 kJ/mol) of 6Zn/SDS system indicated the stability and spontaneity of the system. The position of the zinc complex molecules in various regions of the SDS micelles was determined from the values of partitioning coefficients. The higher value of K_x positions the location of the molecules in the outer zone of the micelles whereas the molecules with the lowest value would stay deep inside the core region as could be witnessed in Scheme 2.
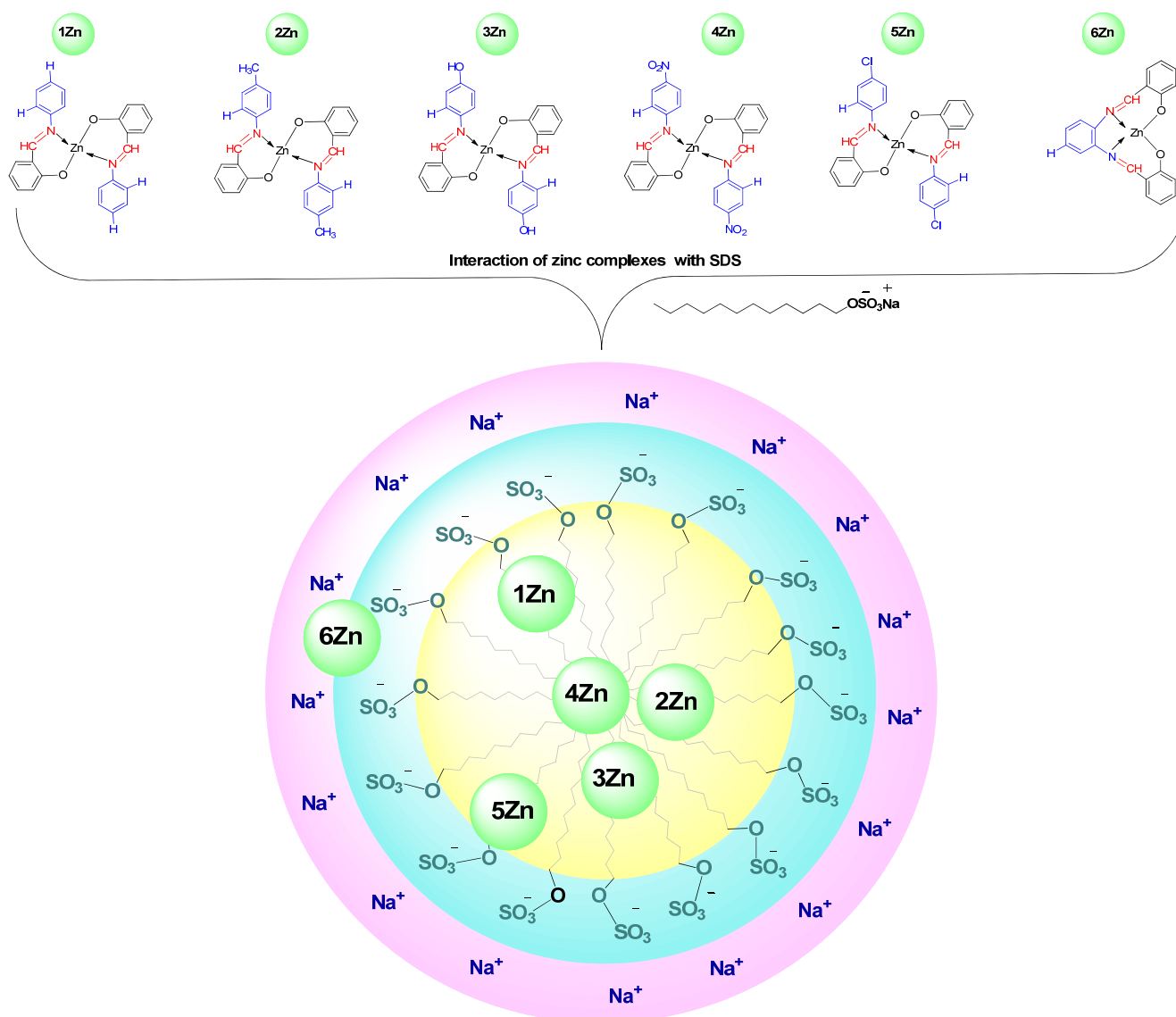
Scheme 2 – Location of zinc complexes in various regions of SDS micelles.

EXPERIMENTAL

Materials and Chemicals

The chemicals used for synthesis were polyethylene glycol (PEG$_{400}$), salicylaldehyde, aniline, p-toluidine, 4-aminophenol, 4-nitroaniline, 1,2-diaminobenzene, 1,4-diaminobenzene, Zinc acetate dehydrate, an anionic surfactant, sodium dodecyl sulphate (SDS) and the solvents methanol and chloroform, purchased from Fluka (Switzerland), Sigma Aldrich (Germany), E-Merck (Germany). All solvents were used without further purification. Elemental analysis was performed by Perkin-Elmer CHNS elemental analyser. The FTIR spectral data were recorded on Bio-Rad Merlin spectrophotometer using KBr discs. The ^{1}HNMR (300MHz) and ^{13}C NMR (75.43 MHz) spectra were recorded on Bruker AM-250 spectrometers in CDCl$_3$, solution using TMS as an internal standard. TG curves were obtained by Perkin-Elmer TGA 7 simultaneous thermal analyser. UV-visible absorption spectra were recorded on Perkin-Elmer Lambda-20 UV-visible spectrophotometer from 200-800nm range. Photoluminescence spectra were recorded on Perkin-Elmer LS 55 luminescence spectro-photometer.

General procedure for the synthesis of ligands (L1-L6)

The substituted aniline (0.01 mol) and salicylaldehyde (0.01 mol) were added in a hot stirred solution of PEG-400 (40 ml) followed by a few drops of 5% HCl solution. The mixture was refluxed for one hour and then placed in an ice-water bath until the formation of precipitates. The products were filtered, washed, dried, and recrystallized from warm ethanol to get the pure aldimine ligands.

2-((phenylimino)methyl)phenol **(L1)**

Yellow ppt. 75 %. mp 55°C; IR spectrum, υ, cm^{-1}: 3430 (OH), 3051 (=C-H arom.), 1615 (C=N), 1530, 1480 (C=C arom.), 1273 (C-O); ^{1}H-NMR spectrum (300 MHz, DMSO-d$_6$) δ$_H$, ppm: 6.95-6.99 (J=7.8 Hz, 1H, m), 7.04-7.07 (1H, d), 7.28-7.33 (3H, m), 7.38-7.48(4HAr, m), 8.65 (1H, ammine, s), 13.30 (1H, phenolic, s); ^{13}C-NMR spectrum (75 MHz, DMSO-d$_6$) δ$_C$, ppm: 117.27, 148.51, 161.13, 162.70; Calculated, %: C 79.17; H 5.62; N 7.10. C$_{13}$H$_{11}$NO (197.24). Found, %: C 80.02; H 5.03; N 7.92.

2-((p-tolylimino)methyl)phenol **(L2)**

Bright yellow ppt. 86 %. mp 96°C; IR spectrum, υ, cm^{-1}: 3436 (OH), 3031 (=C-H arom.), 2950 (C-H sp^3), 1615 (C=N), 1561, 1498 (C=C arom.), 1278 (C-O); ^{1}H-NMR spectrum (300 MHz, DMSO-d$_6$) δ$_H$, ppm: 2.41 (3H, CH$_3$, s), 6.94-6.99 (J=7.8 Hz, 1H, m), 7.04-7.06 (1H, d), 7.21-7.28 (4H, m), 7.30-7.42 (2HAr, m), 8.64 (1H, ammine, s), 13.43 (1H, phenolic, s); ^{13}C-NMR spectrum (75 MHz, DMSO-d$_6$) δ$_C$, ppm: 161.12, 161.72; Calculated, %: C 79.59; H 6.20; N 6.63. C$_{14}$H$_{13}$NO (211.26). Found, %: C 80.21; H 7.06; N 6.76.

2-(((4-hydroxyphenyl)imino)methyl)phenol **(L3)**

Red ppt. 72 %. mp 143-144°C; IR spectrum, υ, cm^{-1}: 3436 (OH), 3031 (=C-H arom.), 1614 (C=N), 1503, 1453 (C=C arom.), 1255 (C-O); ^{1}H-NMR spectrum (300 MHz, DMSO-d$_6$) δ$_H$, ppm: 6.90-6.98 (J=7.8 Hz, 1H, m), 7.03-7.05 (1H, d), 7.23-7.28 (2H, m), 7.35-7.41 (2HAr, m), 8.62 (1H, ammine, s), 13.43 (1H, phenolic, s); ^{13}C-NMR spectrum (75 MHz, DMSO-d$_6$) δ$_C$, ppm: 116.16-141.36, 154.95, 160.49, 160.98; Calculated, %: C 77.23; H 5.20; N 6.57. C$_{13}$H$_{11}$NO$_2$ (213.24). Found, %: C 77.21; H 4.64; N 6.01.

2-(((4-nitrophenyl)imino)methyl)phenol **(L4)**

Orange ppt. 70 %. mp 160-161°C; IR spectrum, υ, cm^{-1}: 3466 (OH), 3046 (=C-H arom.), 1604 (C=N), 1509, 1458 (C=C arom.), 1338, 1508 (NO$_2$), 1269 (C-O); ^{1}H-NMR spectrum (300 MHz, DMSO-d$_6$) δ$_H$, ppm: 6.98-7.03 (J=8.1Hz, 1H, m), 7.05-7.08 (1H, d), 7.36-7.41 (2H, m), 7.44-7.50 (2HAr, m), 8.29-8.34 (2H, m), 8.65 (1H, ammine, s), 12.59 (1H, phenolic, s); ^{13}C-NMR spectrum (75 MHz, DMSO-d$_6$) δ$_C$, ppm: 117.55-154.21, 161.33, 165.41; Calculated, %: C 64.46; H 4.16; N 11.56. C$_{13}$H$_{10}$N$_2$O$_3$ (242.23). Found, %: C 64.21; H 4.41; N 10.89.

2-(((4-chlorophenyl)imino)methyl)phenol **(L5)**

Grey ppt. 60 %. mp 134-136°C; IR spectrum, υ, cm^{-1}: 3467 (OH), 3045 (=C-H arom.), 1609 (C=N), 1519, 1460 (C=C arom.), 1260 (C-O); ^{1}H-NMR spectrum (300 MHz, DMSO-d$_6$) δ$_H$, ppm: 6.96-7.04 (J=8.1Hz, 1H, m), 7.06-7.09 (1H, d), 7.33-7.39 (2H, m), 7.40-7.47 (2HAr, m), 8.22-8.35 (2H, m), 8.67 (1H, ammine, s), 12.50 (1H, phenolic, s); ^{13}C-NMR spectrum (75 MHz, DMSO-d$_6$) δ$_C$, ppm: 116.42-153.33, 162.34, 166.31; Calculated, %: C 67.40; H 4.35; N 6.05. C$_{13}$H$_{10}$ClNO (231.68). Found, %: C 68.29; H 3.96; N 6.71.

2-(((2-aminophenyl)imino)methyl)phenol **(L6)**

Yellow ppt. 80 %. mp 163-164°C; IR spectrum, υ, cm^{-1}: 3450 (OH), 3051 (=C-H arom.), 1609 (C=N), 1560, 1479 (C=C arom.), 1274 (C-O); ^{1}H-NMR spectrum (300 MHz, DMSO-d$_6$) δ$_H$, ppm: 6.92-6.97 (J=8.1Hz, 1H, m), 7.06-7.09 (1H, d), 7.24-7.28 (2H, m), 7.35-7.42 (2HAr, m), 8.65 (1H, ammine, s), 13.08 (1H, phenolic, s); ^{13}C-NMR spectrum (75 MHz, DMSO-d$_6$) δ$_C$, ppm: 117.58-142.58, 163.73, 166.36; Calculated, %: C 75.93; H 5.10; N 8.86. C$_{20}$H$_{16}$N$_2$O$_2$ (316.36). Found, %: C 76.57; H 9.02; N 8.88.

General procedure for the synthesis of Zn(II) complexes (1Zn-6Zn)

15 mL of methanolic solutions of zinc acetate dihydrate (0.01 mol) and 15 mL of aldimine ligand (0.01 mol) were mixed in a 100 mL flask equipped with a reflux condenser fitted in the domestic microwave oven. The mixture was heated at 150 °C for 20 minutes. The precipitates were filtered and washed with methanol to get the amorphous product. Unfortunately, no crystalline products suitable for single crystal XRD analysis were obtained.

Zn(2-((phenylimino)methyl)phenol)$_2$ **(1Zn)**

Yellowish green solid. 83 %. mp 184-186°C; IR spectrum, υ, cm^{-1}: 3051 (=C-H arom.), 1604 (C=N), 1531, 1484 (C=C arom.), 1251 (C-O), 537 (Zn-O), 488 (Zn-N); ^{1}H-NMR spectrum (300 MHz, DMSO-d$_6$) δ$_H$, ppm: 6.96-6.98 (J=7.7Hz, 1H, m), 7.06-7.08 (1H, d), 7.38-7.43 (1HAr, m), 8.37 (1H, ammine, s); ^{13}C-NMR spectrum (75 MHz, DMSO-d$_6$) δ$_C$, ppm: 115-162, 169, 171; Calculated, %: C 68.21; H 4.40; N 6.12. C$_{26}$H$_{20}$N$_2$O$_2$Zn (457.84). Found, %: C 69.58; H 4.06; N 6.48.

Zn(2-((p-tolylimino)methyl)phenol)$_2$ **(2Zn)**

Yellowish solid, 73 %. mp 191-193°C; IR spectrum, υ, cm^{-1}: 3031 (=C-H arom.), 2990 (C-H sp^3), 1585 (C=N), 1527, 1448 (C=C arom.), 1250 (C-O), 584 (Zn-O), 500 (Zn-N); ^{1}H-NMR spectrum (300 MHz, DMSO-d$_6$) δ$_H$, ppm: 2.29 (3H, s), 6.64-6.70 (J=7.7Hz, 1H, m), 6.94-7.08 (5H, m), 7.20-7.23 (1H, q), 7.36-7.41 (1Har, m), 8.37 (1H, ammine, s); ^{13}C-NMR spectrum (75 MHz, DMSO-d$_6$) δ$_C$, ppm: 21.11, 115.11-161.73, 169.05, 171.17; Calculated, %: C 69.2; H 4.98; N 5.77. C$_{28}$H$_{24}$N$_2$O$_2$Zn (485.89). Found, %: C 68.49; H 4.35; N 5.87.

Zn(2-(((4-hydroxyphenyl)imino)methyl)phenol)$_2$ **(3Zn)**

Yellowish solid, 73 %. mp 191-193°C; IR spectrum, υ, cm^{-1}: 3019 (=C-H arom.), 1594 (C=N), 1509, 1438 (C=C arom.), 1276 (C-O), 587 (Zn-O), 501 (Zn-N); ^{1}H-NMR spectrum (300 MHz, DMSO-d$_6$) δ$_H$, ppm: 3.17 (1H, s), 6.61-6.72 (J=7.13Hz, 4H, m), 7.12-7.15 (J=7.32, 2H, d), 7.30-7.35

(J=7.48, 1H, t), 7.48-7.49 (1HAr, d), 8.71 (1H, ammine, s); ¹³C-NMR spectrum (75 MHz, DMSO-d₆) δ_C, ppm: 115.02-157.08, 168.65, 170.65; Calculated, %: C 63.75; H 4.12; N 5.72. C₂₆H₂₀N₂O₄Zn (489.84). Found, %: C 63.21; H 4.06; N 5.88.

Zn(2-(((4-nitrophenyl)imino)methyl)phenol)₂ **(4Zn)**

Orange shiny powder. 85 %. mp >300°C; IR spectrum, υ, cm⁻¹: 3046 (=C-H arom.), 1599 (C=N), 1508, 1451 (C=C arom.), 1324 (NO₂), 1254 (C-O), 583 (Zn-O), 415 (Zn-N); ¹H-NMR spectrum (300 MHz, DMSO-d₆) δ_H, ppm: 7.01-7.09 (J=7.42Hz, 2H, q), 7.38-7.47 (J=8.33, 4H, q), 8.32-8.34 (2HAr, d), 8.65 (1H, ammine, s); ¹³C-NMR spectrum (75 MHz, DMSO-d₆) δ_C, ppm: 117.55-154.21, 161.33, 165.41; Calculated, %: C 57.00; H 3.31; N 10.23. C₂₆H₁₈N₄O₆Zn (547.83). Found, %: C 48.91; H 3.06; N 10.18.

Zn(2-(((4-chlorophenyl)imino)methyl)phenol)₂ **(5Zn)**

Grey solid. 80 %. mp >300°C; IR spectrum, υ, cm⁻¹: 3014 (=C-H arom.), 1587 (C=N), 1567, 1450 (C=C arom.), 1251 (C-O), 532 (Zn-O), 476 (Zn-N); ¹H-NMR spectrum (300 MHz, DMSO-d₆) δ_H, ppm: 6.59-6.66 (J=6.33Hz, 1H, t), 6.71-6.74 (J= 6.71Hz, 1H, d) 7.25-7.31 (1H, m), 7.45-7.52 (2H, m), 7.89-7.94 (1HAr, m), 8.45 (1H, ammine, s); ¹³C-NMR spectrum (75 MHz, DMSO-d₆) δ_C, ppm: 113.32-120.32, 165.19, 170.75; Calculated, %: C 59.29; H 3.44; N 5.32. C₂₆H₁₈N₂O₂Cl₂Zn (526.72). Found, %: C 58.98; H 5.26; N 5.28.

Zn(2-(((2-aminophenyl)imino)methyl)phenol) **(6Zn)**

Orange shiny powder. 83 %. mp >300°C; IR spectrum, υ, cm⁻¹: 3004 (=C-H arom.), 1596 (C=N), 1577, 1448 (C=C arom.), 1243 (C-O), 523 (Zn-O), 488 (Zn-N); ¹H-NMR spectrum (300 MHz, DMSO-d₆) δ_H, ppm: 6.49-6.54 (J=6.51Hz, 1H, t), 6.69-6.72 (J= 6.71Hz, 1H, d) 7.15-7.30 (1H, m), 7.35-7.50 (2H, m), 7.88-7.91 (J=7.9Hz, 1HAr, q), 9.01 (1H, ammine, s); ¹³C-NMR spectrum (75 MHz, DMSO-d₆) δ_C, ppm: 113.42-119.83, 163.29, 172.73; Calculated, %: C 63.26; H 3.72; N 7.38. C₂₀H₁₄N₂O₂Zn (379.72). Found, %: C 63.46; H 3.62; N 7.48.

The overall synthesis route form ligands to zinc complexes are given in Scheme 1.

Anti-inflammatory studies

Anti-inflammatory studies were carried out for the aldimine and Zn(II) complexes by minor modification of the bovine serum albumin (BSA) denature inhibition technique.[17] "The synthesized aldimine and their Zn(II) complexes were administered with the standard drug diclofenac sodium taken at different doses of 10 mM, 50 mM, 100 mM, 250 mM and 500 mM dissolved in water and dimethylformamide (DMF) with diluted phosphate buffer (0.2 M, pH = 7.4). About 4 mL of the obtained minimum concentration (less than 2.5%) of all test solutions was mixed with 1 mL of 1 mM bovine serum albumin solution in phosphate buffer. Further, the mixture was kept in an incubator at 37 °C for 20 min and denaturation was kept by keeping the reaction mixture at 70 °C in a water bath for 30 min; then, it could cool to room temperature and measured at 660 nm using UV/Visible spectrophotometry. The percentage of denaturing inhibition was measured for the control without the addition of drug and diclofenac sodium was employed as a standard drug. The percentage of albumin denature inhibition was calculated using Equation 1.

$$Albumin\ denature\ inhibition\ (\%) = \left[1 - \frac{A_c}{A_t}\right] \times 100 \quad (Eq.\ 1)$$

where A_c and A_t represent optical density (O.D.) of the test solution and control, respectively."
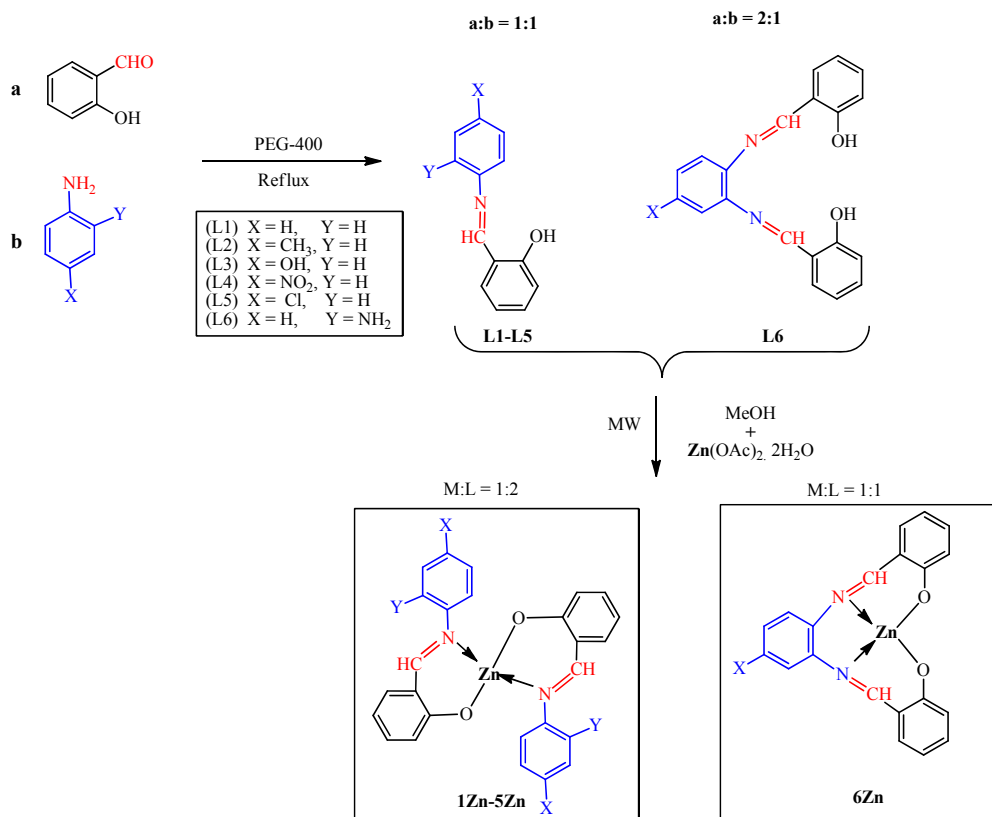
Scheme 1 – Synthesis of aldimine ligands and their corresponding zinc complexes.

Procedure for preparation of solution for solubilization studies

The solutions of the complexes (1Zn-6Zn) were prepared in distilled deionized water to investigate their conductometric and spectroscopic parameters. The aqueous solution of zinc complexes was the primary solution and it was further used for the preparation of secondary solutions by dissolving SDS (7–15 mM) in pre-micellar, micellar, and post-micellar concentrations[18].

Apparatus and methods for solubilization studies

UV-Visible spectroscopy

UV-Visible absorbance values of aqueous solutions of zinc complexes (1 mM each) in the presence and absence of SDS were measured on computer interfaced double beam UV-Visible spectrophotometer (Perkin Elmer, USA). The extent and nature of the interaction between complex molecules and surfactant were revealed by measuring simple and differential absorbance value recorded in square quartz cells (10 mm thick; 1 nm slit width) at 298K with accuracy control of ±0.5K. In recording differential absorbance, the aqueous solution of Zn complex (8.2 mM) was used as reference and solution of zinc complex in the presence of SDS was used in the sample cell. This absorbance data was used to measure the partitioning and binding parameters of solubilization. The equations for calculating these parameters are presented in equations 3–6.

Partition and Binding Parameters

The distribution of zinc complexes between aqueous and micellar media was governed by Partition law as proposed by Kawamura et al. to calculate partitioning coefficients using differential UV/Visible absorbance method.[19]

The differential absorbance (ΔA) was calculated using with relationship presented in equation 3.

$$\frac{1}{\Delta A} = \frac{1}{K_C \Delta A_\infty (C_a + C_S^{m0})} + \frac{1}{\Delta A_\infty} \qquad \text{(Eq. 3)}$$

In Equation 5: K_c is the partition constant; C_a for concentration of zinc complexes; ΔA_∞ is the value differential absorbance at infinite dilution. In the relationship $C_S^m = C_s - \text{CMC}_o$; CMC_o is the CMC of SDS in aqueous medium and C_s is representing the concentration of SDS used. Partitioning coefficient (K_x) was calculated from the given expression, n_w = number of moles of water. The standard change in free energy of partition) $\left(\Delta G_p\right)$ was calculated with equation 4 whereas, the binding constant (K_b) was calculated from the equation 5.

$$\Delta G_p = -RT \ln K_x \qquad \text{(Eq. 4)}$$

$$\frac{C_s C_a}{\Delta A} = \frac{C_s}{\Delta \in 1} + \frac{1}{K_b \Delta \in 1} \qquad \text{(Eq. 5)}$$

C_a is representing the concentration of the metal complex. The standard binding free energy change (ΔG_b) was computed from equation 6.

$$\Delta G_b = -RT \ln K_b \qquad \text{(Eq. 6)}$$

Electrical conductivity (EC)

Electrical conductivity parameters were studied with Hanna Cond. meter (HI-99301) at varying temperatures from 298 to 318 K (10 K increment rate) with accuracy maintenance up to ±0.5% and ~ ±0.5 K. The electrodes of the conductometer were coated with platinum black to avoid any possible polarizations and to measure conductivity in 0.01–199.9 mS range. The electrode was calibrated with KCl solution in the required concentration range from molar conductivity data.

Thermodynamic Parameters

This conductivity data was used to measure thermodynamic parameters of solubilization. The equations for calculating these parameters are presented equations 7-10.

(i) The extent of dissociation (β)

The ratio of the slopes of straight lines in the post-micellar and pre-micellar regions as shown in equation 7 gave the value of β.

$$\beta = \frac{S_{2(Post-micellar\ slope)}}{S_{1(Pre-micellar\ slope)}} \qquad \text{(Eq. 7)}$$

(ii) Free energy of micellization $\left(\Delta G_m^0\right)$ was computed by Eq. 8.

$$\Delta G_m^0 = \left(2 - \beta\right) RT \ln X_{CMC} \qquad \text{(Eq. 8)}$$

(iii) Entropy of micellization $\left(\Delta S_m\right)$ was calculated using equation 9.

$$\Delta S_m = \frac{\Delta H_m - \Delta G_m^0}{T} \qquad \text{(Eq. 9)}$$

(iv) Enthalpy of micellization $\left(\Delta H_m\right)$ was computed with help of the following equation 10.

$$\Delta H_m = -2.3(22\beta)RT^2 \left[\frac{\partial(\log X_{CMC})}{\partial T}\right]_P \qquad \text{(Eq. 10)}$$

In the above equations: β: degree of dissociation, X_{CMC}: mole fraction of surfactants at CMC R : universal gas constant (~8.314Jmol⁻¹K⁻¹); T : absolute temperature.

The values of CMC of surfactant and thermodynamic parameters are summarized in Table 5.

CONCLUSIONS

A series of amorphous Zn(II) complexes with aldimines derived from salicylaldehyde were synthesized and characterized. The aldimine acts as a bidentate ligand and coordinated to zinc metal

through oxygen and azomethine nitrogen so the tetrahedral structure of complexes has been proposed. The coordination of ligand to Zn(II) ion confirmed by spectral studies (UV-Vis, FT-IR, ^{1}H and ^{13}C NMR, photoluminescence), elemental and thermal (TGA, DTG). The complexes showed strong blue-green emission upon UV irradiation in solid-state and in solution forms. The optical absorption data of the complexes was employed to determine the optical band gaps in the range of 2.35-3.90 eV representing good optical properties. The anti-inflammatory studies proved that the aldimines were found to be biologically active and their Zn(II) complexes show meaningfully greater anti-inflammatory activity as compared to the free ligands. Thus, after analysing their toxicity to human beings, their vast nature can be additionally beneficial to the pharmaceutical industry, as an anti-inflammation agent. The solubilization of these complexes in sodium dodecyl sulphate (SDS) was also investigated. The thermodynamic parameters including free energy, enthalpy, and entropy of micellization were determined by electrical conductivity. The interaction of zinc complexes with sodium dodecyl sulphate (SDS) was studied with the help of UV-Visible spectroscopy and electrical conductivity. We claim to pioneer such micellar interactions of zin-aldimine complexes. Partition and binding constants, their corresponding free energies were investigated through simple and differential spectroscopy. The values of critical micellar concentration CMC obtained from UV/Visible spectroscopy and conductometry were found in close agreement.

REFERENCES

1. M. M. Shakdofa, M. H. Shtaiwi, N. Morsy and T. Abdel-Rassel, *Main Group Chem.,* **2014**, *13*, 187-218.
2. J. Y. Mak, W. Xu, R. C. Reid, A. J. Corbett, B. S. Meehan, H. Wang, Z. Chen, J. Rossjohn, J. McCluskey and L. Liu, *Nature Comm.,* **2017**, *8*, 1-13.
3. S. Gomez-Coca, E. Cremades, N. Aliaga-Alcalde and E. Ruiz, *J. Am. Chem. Soc.,* **2013**, *135*, 7010-7018.
4. M. Pan, B. B. Du,Y. X. Zhu, M. Q. Yue, Z. W. Wei and C. Y. Su, *Chem.–A Euro. J.,* **2016**, *22*, 2440-2451.
5. M. M. Abd-Elzaher, A. A. Labib, H. A. Mousa, S. A. Moustafa, M. M. Ali and A. A. El-Rashedy, *Beni-Suef Univ. J. Basic Appl. Sci.,* **2016**, *5*, 85-96.
6. W. Zishen, L. Zhiping and Y. Zhenhuan, *Trans. Metal Chem.,* **1993**, *18*, 291-294.
7. E. Yousif, A. Majeed, K. Al-Sammarrae, N. Salih, J. Salimon and B. Abdullah, *Arab. J. Chem.,* **2017**, *10*, S1639-S1644.
8. M. Azam, S. I. Al-Resayes, A. Trzesowska-Kruszynska, R. Kruszynski, F. Shakeel, S. M. Soliman, M. Alam, M. R. Khan and S. M. Wabaidur, *J. Molec. Struct.,* **2020**, *1201*, 127177.
9. C. Maxim, T. D. Pasatoiu, V. C. Kravtsov, S. Shova, C. A. Muryn, R. E. Winpenny, F. Tuna and M. Andruh, *Inorg. Chim. Acta,* **2008**, *361*, 3903-3911.
10. O. Kotova, S. Eliseeva, A. Averjushkin, L. Lepnev, A. Vaschenko, A. Y. Rogachev, A. Vitukhnovskii and N. Kuzmina, *Russ. Chem. Bull.,* **2008**, *57*, 1880-1889.
11. G. Kumaravel, P. P. Utthra and N. Raman, *Bioorg. Chem.,* **2018**, 77, 269.
12. L. Armelao, S. Quici, F. Barigelletti, G. Accorsi, G. Bottaro, M. Cavazzini and E. Tondello, *Coord. Chem. Rev.,* **2010**, *254*, 487-505.
13. R. Raciti, R. Bahariqushchi, C. Summonte, A. Aydinli, A. Terrasi and S. Mirabella, *J. Appl. Phys.,* **2017**, *121*, 234304.
14. L. Viganor, O. Howe, P. McCarron, M. McCann and M. Devereux, *Curr. Top. Med. Chem.,* **2017**, *17*, 1280-1302.
15. N. Raman, R. Jeyamurugan and J. Joseph, *J. Iran. Chem. Res.,* **2010**, *3*, 83-95.
16. P. Nisar, N. Ali, L. Rahman, M. Ali and Z. K. Shinwari, *J. Bio. Inorg. Chem. (JBIC),* **2019**, *24*, 929-941.
17. M. Amiri, D. Ajloo, M. Fazli, A. Mokhtarieh, G. Grivani JBIC A. A. Saboury, *J. Biomolec. Struct. Dynamics,* **2018**, *36*, 3753-3772.
18. M. B. Taj, M. D. Alkahtani, U. Ali, A. Raheel, W. Alelwani, A. M. Alnajeebi, N. A. Babteen, S. Noor and H. Alshater, *Molecules,* **2020**, *25*, 4252.
19. M. Taj, A. Raheel, W. Alelwani, D. Hajjar, A. Makki, A. Alnajeebi, N. Babteen, S. Tırmizi and S. Noor, *Russ. J. Gen. Chem.,* **2020**, *90*, 1533-1543.